Pure Appl. Chem., Vol. 76, No. 1, pp. 231–240, 2004.

Calculation of the free energy of solvation from molecular dynamics simulations*

Paulo F. B. Gonçalves and Hubert Stassen‡

Grupo de Química Teórica, Instituto de Química, Universidade Federal do Rio Grande do Sul, 91540-000 Porto Alegre-RS, Brazil

Abstract: Molecular dynamics simulation has been employed in the computation of the free energy of solvation for a large number of solute molecules with different chemical functionalities in the solvents water, acetonitril, dimethyl sulfoxide, tetrahydrofuran, and carbon disulfide. The free solvation energy has been separated into three contributions: the work necessary to create a cavity around the solute in the solvent, the electrostatic contribution, and the free energy containing the short-range interactions between solute and solvent molecules. The cavitational contribution was computed from the Claverie–Pierotti model applied to excluded volumes obtained from nearest-neighbor solute–solvent configurations treating the solvent molecules as spherical. The electrostatic term was calculated from a dielectric continuum approach with explicitly incorporating the solvent's partial charges. The short-range contribution to the free solvation energy was obtained from the force field employed in the simulations. For solutions with available experimental data for the free energy of solvation, we found a satisfactory agreement of the computed free solvation energies and the experimental data set.

INTRODUCTION

The free energy of solvation ΔG_{solv} represents a very important property for the thermodynamical description of a solution with impact in the chemical, biological, and pharmaceutical sciences. From the theoretical point of view, several approaches have been developed to predict ΔG_{solv}. Quite generally, the theories concerning the solvation process can be classified by explicitly or implicitly taking into account the solvent molecules. In the implicit treatment of the solvation process, the solvent is represented by a dielectric continuum in which the solute is embedded, whereas the explicit description of the solvation considers particularities of the real liquid configuration.

The choice of a distinct model for the solvation process depends on the compromise between computational cost and accuracy in the desired property. Implicit solvation models are computationally fast and can be applied to quantum mechanical calculations for the dissolved solute by a perturbation formalism permitting the elucidation of quantum chemical properties in solution. Typical examples for this methodology are described by several recent reviews [1]. On the other hand, explicit solvation models are more rigorous. However, considering explicitly the solvent molecules, the lower computational efficiency limits the practical application to those properties that are available from classical simulation studies of the solvation process. In this context, one might cite solvation studies based on free-energy perturbation [2] or thermodynamic integration [3] that are coupled to molecular dynamics (MD) or Monte Carlo computer simulations.

---

*Lecture presented at the European Molecular Liquids Group (EMLG) Annual Meeting on the Physical Chemistry of Liquids: Novel Approaches to the Structure, Dynamics of Liquids: Experiments, Theories, and Simulation, Rhodes, Greece, 7–15 September 2002. Other presentations are published in this issue, pp. 1–261.
‡Corresponding author: E-mail: gullit@iq.ufrgs.br

In the present manuscript, we combine the explicit treatment of solvation with some basic ideas usually involved in implicit solvation models. This approach to ΔG_{solv} has been described in details previously [4,5] and is here further explored by incorporating the solvents tetrahydrofuran (THF), dimethyl sulfoxide (DMSO), carbon disulfide (CS_2), and acetonitril. Also, additional results for the solvent water are presented. Therefore, MD simulations on diluted solutions of solutes with different chemical functionalities in these solvents have been performed. From the trajectories, we have computed ΔG_{solv} separated into a cavitational contribution, an electrostatic term, and a short-range portion containing the van der Waals-like interactions between solute and solvent molecules.

In the next section, we introduce briefly the theoretical essentials in our approach to the free energy of solvation. It is not our purpose to enter here into all the theoretical and algorithmic details of the procedures involved in the computation of ΔG_{solv}. However, in order to discuss the possibilities and limitations of our method, we briefly review some basic assumptions of our approach in the theoretical section. More theoretical and algorithmic information can be found in ref. [5]. Afterwards, the computational details of the MD simulations are summarized. Results are presented and critically discussed, before finishing the article with some conclusive remarks.

THEORETICAL BACKGROUND

The possibility of studying an experimental property separated into partial contributions not accessible by experiment is one of the motivations for performing computer simulations. In the case of the free energy of solvation, three distinct physical contributions to ΔG_{solv} can be sorted out [6]: (i) the free-energy ΔG_{cav} for the creation of the excluded volume for the solvent S around the solute M, (ii) the free-energy ΔG_{el} related to the formation of electrostatic interactions between M and S, and (iii) a short-range free-energy ΔG_{sr} containing the repulsive and attractive van der Waals-like interactions between M and S,

$$\Delta G_{solv} = \Delta G_{cav} + \Delta G_{el} + \Delta G_{sr}. \tag{1}$$

In eq. 1, we assume that the solute's Born–Oppenheimer surface for the gas phase is maintained in the liquid phase and that the solute's partition function for nonelectronic degrees of freedom are not changed when introducing M into S. Especially in the case of the translational partition function, this assumption is only justified when the accessible volume for the solute in solution corresponds to the gas-phase volume. Otherwise, a so-called liberation term has to be added to eq. 1 [7].

In the following, we are considering a given configuration for the solution of one molecule M in N molecules of S. The cavity around M is created assuming the solvent molecules as spherical (not in the simulations, but only in the cavity creation). Each of the solute's atoms is represented by a sphere of radius r_i. Particularities of the liquid state are included by defining r_i as the geometric mean of the distance between the i-th solute's atom to the nearest center of mass of a solvent molecule. Afterwards, the GEPOL algorithm [8] is applied to the solute described by its set of spheres with radii r_i. Smaller spheres (with a minimum radius of 0.01 Å) are added to interspherical contact regions. Removing the overlap between spheres, the surface area A_i is obtained for each sphere. The sum of all the A_is defines the solvent accessible surface area of the solute.

The corresponding cavitational free energy can be computed as the sum over the solute's N_s spheres with cavitational free energies $\Delta G_{cav,i}$ weighted by its solvent accessible surface area fraction [9],

$$\Delta G_{cav} = \sum_{i=1}^{N_S} \frac{A_i}{4\pi r_i^2} \Delta G_{cav,i}, \tag{2}$$

with $\Delta G_{cav,i}$ defined from the scaled particle theory [10] as the cavitation free energy for a sphere with radius r_i dissolved in a solvent composed by spheres with radii r_s. Note that the partial $\Delta G_{cav,i}$ depend

in addition to the size of solvent molecules on the thermodynamic state defined by temperature, pressure (1 atm), and number density of the solvent.

In order to compute the electrostatic free energy ΔG_{el}, the solute's cavity created as described above has been used. Therefore, we divided the surfaces of each sphere belonging to the solute into 60 tessera. An apparent surface charge (ASC) distribution is obtained by projecting the solute's point charges onto the center of each tesserae belonging to the solvent accessible surface area. The interaction between the ASCs q_i defines the electrostatic gas-phase free-energy G_0,

$$G_0 = \sum_i q_i V_{mol}, \tag{3}$$

where we have used V_{mol} in order to express the electrostatic potential emanated by all the other ASCs.

Bringing the ASCs into the liquid phase, a charge reorganization process is initiated due to additional electrostatic potentials stemming from the solvent. In our approach [5], the solvent is represented by a dielectric continuum with dielectric constant ε. In order to account empirically for some anisotropy and distance dependence in ε, we added the external potential V_{ext} from all the solvent's point charges. Thus, as a result, the reorganized ASCs can be computed by [5]

$$q_i = -\frac{\varepsilon - 1}{4\pi\varepsilon} \frac{\partial\left[V_{ext}(\mathbf{r}) + V_{mol}(\mathbf{r})\right]}{\partial \hat{\mathbf{p}}_i} A_i \tag{4}$$

The new ASCs, q_i, give rise to a different molecular potential V_{mol}. As shown in ref. [5], a self-consistent iteration scheme applied to the q_i reaches rapidly convergency. The resulting q_i, corrected by requirement that the ASC distribution corresponds to a neutral molecule, is used to compute the electrostatic free energy [5],

$$\Delta G_{el} = \sum_i q_i' V_{mol}' - G_0, \tag{5}$$

with the prime indicating liquid-state properties.

The short-range contribution ΔG_{sr} due to van der Waals-like interactions of the solute and the solvent is calculated from the nonelectrostatic interactions as defined by the force field applied to the simulations. Following Floris et al. [15], ΔG_{sr} is written as the average for the nonelectrostatic interactions between the solute and the solvent molecules,

$$\Delta G_{sr} = \frac{1}{N} \sum_{\alpha} \sum_{i=1}^{N} \sum_{\beta} u_{\alpha\beta}\left(r_{\alpha\beta}\right), \tag{6}$$

where $r_{\alpha\beta}$ is the distance between the atom α of the solute and the atom β of the i-th solvent molecule interacting by the pair potential $u(r_{\alpha\beta})$.

The three contributions to ΔG_{solv} as defined by the eqs. 2, 5, and 6 can easily be sampled as an experimental average along a trajectory for the solution created by MD simulations. For a detailed discussion of the fluctuations involved in ΔG_{solv} and its contributions from eq. 1 during a MD simulation, we refer to ref. [4].

COMPUTATIONAL DETAILS

MD simulations on diluted solutions (one solute in 255 solvent molecules) have been performed in the NVT ensemble. The molecules were arranged in a cubic box with dimensions corresponding to the experimental densities of the solvents [11]. A spherical cutoff corresponding to half of the cube's side length was employed in the computation of all the distance-dependent properties. The usual periodic boundary conditions and minimum image conventions were applied. Long-range electrostatic interactions were corrected by a standard reaction field [12]. Starting from initial configurations defined by a

randomly perturbed fcc lattice structure with random velocities, several thousands of time steps have been used in order to equilibrate the solution at the desired temperature of 298 K. The equations of motion were resolved with a leap-frog algorithm [13] using a time step of 2×10^{-15} s. The temperature was held constant by the Nosé–Hoover thermostat [14]. Some computational speed up has been achieved by the use of a neighborhood list that was updated in intervals of 10 integration time steps. The production runs were expanded to 120–140 ps. In intervals of 50 time steps, we have sampled the free energy of solvation. The choice of this large interval in the sampling procedure has been adopted in order to compute ΔG_{solv} from configurations that can be considered as statistically independent. In the simulations, all the molecules have been treated as rigid. Thus, in our approximation to ΔG_{solv}, we transferred perfectly the gas-phase geometry of the solute into the liquid phase.

The molecular geometries of the solutes were obtained from ab initio calculations using MP2/augccTVZ basis functions with the Gaussian98revA9 program [16]. Atomic partial charges were computed as ChelpG charges. These charges were employed in the calculation of electrostatic intermolecular interactions. In addition, the ChelpG charges were used as the initial guess for the estimation of the electrostatic contribution to ΔG_{solv}. Nonelectrostatic intermolecular interactions involving the solute molecules were taken from the all-atom OPLS force field [17]. For the solvents, we also have chosen the OPLS force field with the exception of DMSO that has been described by the 4-center Lennard–Jones plus Coulomb potential of van Gunsteren et al. [18], CS_2 that was modeled by the 3-center Lennard–Jones potential of Tildesley and Madden [19], and water that has been treated as SPC/E water [20]. All cross interaction parameters between solutes and solvent molecules were obtained from the Lorentz–Berthelot mixing rules [13].

The charge models as defined by the potential models have also been used in the computation of the external potential $V_{ext}(r)$ from eq. 4. Only in the case of CS_2 described by a charge-free potential model, ChelpG charges were obtained from ab initio calculations at the MP2/aug-ccTVZ level and utilized in the computation of $V_{ext}(r)$.

RESULTS AND DISCUSSION

The solvation free-energy ΔG_{solv} decomposed into the electrostatic, short-range, and cavitational contributions as illustrated by eq. 1 has been calculated from the MD simulations utilizing a large number of configurations along the trajectory for the solutions. Thus, the computed ΔG_{solv} as well as its contributions ΔG_{el}, ΔG_{sr}, and ΔG_{cav} have been accurately averaged for all the solutions. The computation of ΔG_{solv} for a given configuration of the solution was initiated by searching the shortest distances between the solute's atoms and the center of mass of the solvent molecules. These distances have been used to define the excluded volume for the solvent around the solute by the GEPOL algorithm. In terms of pair-distribution functions [21], the averaged excluded volume reflects the first non-zero entry in the pair distribution function for the considered solute's atom and the center of mass of the solvent. As pointed out in the theoretical section, the created cavity representing the solute in the solution has been used in the estimate of ΔG_{el}. The short-range term ΔG_{sr} was computed by averaging all the solute–solvent Lennard–Jones interactions.

In Table 1, we have summarized ΔG_{solv} as well as its contributions ΔG_{cav}, ΔG_{el}, and ΔG_{sr} for 30 solutes dissolved in water. Additionally, experimental free energies of solvation ΔG_{exp} from ref. [22] are included in Table 1. The agreement between the calculated and the experimental free energies of solvation is excellent for all the solutes. From the statistical error in the simulated ΔG_{solv}, it becomes evident that the computed ΔG_{solv} for most of the solutes match the experimental findings within the error bar. The comparison between experimental and computed solvation free energies is also graphically illustrated in Fig. 1. The data points in this figure are spread about the theoretical line for perfect agreement between computed and experimental free energies of solvation. Thus, the calculated ΔG_{solv} are not affected by any systematical deviation from the experimental values.

Table 1 Calculated free energies of solvation ΔG_{solv} and their contributions from eq. 1 for the solvent water. Also given are experimental free energies of solvation ΔG_{exp} [22]. In the calculation of ΔG_{solv}, water is described by $\varepsilon = 78.36$ [11] possessing a radius $r_s = 1.385$ Å [24]. All free energies are in kcal/mol.

Solute	ΔG_{el}	ΔG_{sr}	ΔG_{cav}	ΔG_{solv}	ΔG_{exp}
1,2–Ethanediol	–8.1 ± 0.9	–7.9 ± 0.2	8.3 ± 0.6	–7.7 ± 0.6	–7.7
Acetamide	–10.6 ± 0.5	–10.6 ± 0.3	11.3 ± 0.3	–10.0 ± 0.1	–9.7
Acetophenone	–6.0 ± 0.7	–7.8 ± 0.2	9.9 ± 0.2	–3.8 ± 0.6	–4.6
Acetonitrile	–5.9 ± 0.5	–7.4 ± 0.8	8.1 ± 0.8	–4.4 ± 0.4	–3.9
Butanoic acid	–8.4 ± 0.5	–11.8 ± 0.8	14.1 ± 0.5	–6.2 ± 0.5	–6.4
Ethanoic acid	–7.5 ± 0.3	–9.2 ± 0.3	10.2 ± 0.5	–6.6 ± 0.2	–6.7
Propanoic acid	–7.5 ± 0.9	–7.8 ± 0.7	9.1 ± 0.2	–6.3 ± 0.4	–6.5
Water	–7.4 ± 0.3	–4.1 ± 0.2	4.8 ± 0.2	–6.7 ± 0.3	–6.3
Ammonia	–6.2 ± 0.8	–3.6 ± 0.6	4.6 ± 1.0	–5.2 ± 0.2	–4.3
Benzenethiol	–3.8 ± 0.7	–10.7 ± 0.2	12.6 ± 0.1	–1.9 ± 0.1	–2.6
Cyclohexane	–0.1 ± 0.4	–5.9 ± 0.3	7.8 ± 0.2	1.8 ± 0.3	1.2
Vinyl chloride	–1.9 ± 0.7	–6.7 ± 0.6	8.2 ± 0.4	–0.4 ± 0.2	–0.6
Chloroform	–6.1 ± 0.6	–5.9 ± 0.7	10.0 ± 0.6	–3.0 ± 0.2	–1.1
Methyl chloride	–1.1 ± 0.3	–8.7 ± 0.5	9.1 ± 0.6	–0.7 ± 0.1	–0.6
Dichloromethane	–3.5 ± 0.1	–9.2 ± 0.2	10.8 ± 0.2	–1.9 ± 0.2	–1.4
Dimethylamine	–5.1 ± 0.9	–6.1 ± 0.4	6.6 ± 0.6	–4.6 ± 0.4	–4.3
1,4–Dioxan	–7.3 ± 0.94	–8.3 ± 0.9	10.9 ± 0.3	–4.8 ± 0.4	–5.1
E–Dichloroethene	–4.9 ± 0.7	–4.3 ± 0.3	7.4 ± 0.2	–1.8 ± 0.8	–0.8
Ethanol	–6.4 ± 0.6	–7.1 ± 1.0	9.3 ± 0.2	–4.3 ± 0.5	–5.0
Glycerol	–11.9 ± 0.5	–6.5 ± 0.9	10.5 ± 0.7	–7.9 ± 1.0	–9.1
Methanol	–6.8 ± 0.3	–6.4 ± 0.2	8.1 ± 0.4	–5.1 ± 0.1	–5.1
Methanethiol	–3.8 ± 0.2	–8.5 ± 0.2	11.4 ± 0.3	–0.9 ± 0.3	–1.2
Methylamine	–5.9 ± 0.3	–8.5 ± 0.2	9.6 ± 0.3	–4.8 ± 0.2	–4.6
Dimethyl ether	–2.5 ± 0.7	–11.5 ± 0.6	11.3 ± 0.6	–2.7 ± 0.1	–1.9
Neopentane	0.0 ± 0.6	–14.4 ± 0.4	16.1 ± 0.8	1.6 ± 0.6	2.5
n–propanol	–6.7 ± 0.4	–6.8 ± 0.5	9.2 ± 0.8	–4.3 ± 0.3	–4.8
Propane	–0.1 ± 0.1	–5.4 ± 0.7	6.9 ± 0.7	1.5 ± 0.2	2.0
Tetrahydrofuran	–4.3 ± 0.2	–14.8 ± 1.0	15.3 ± 0.7	–3.8 ± 0.4	–3.5
Thiophenol	–4.1 ± 0.3	–12.0 ± 0.5	14.2 ± 0.7	–1.9 ± 0.1	–2.6
Trichloroethane	–1.1 ± 0.4	–6.5 ± 0.5	8.1 ± 0.5	0.5 ± 0.2	–0.3

The observed agreement between the experimental and calculated free energies of solvation in the solvent water justifies the approximations involved in the theoretical pathway to ΔG_{solv}. The water molecule is sufficiently spherical, or at least, does not exhibit larger anisotropies in its molecular shape that contradict the spherical approximation to the solvent molecule in the cavitational process. In addition, the large dielectric constant for liquid water turns the factor $(\varepsilon - 1)/\varepsilon$ in eq. 4 almost equal to one and, thus, facilitates the balancing of possible dielectric anisotropies by the external potential $V_{ext}(r)$ in the electrostatic portion ΔG_{el}. However, ΔG_{el} depends on the size and shape of the created cavity. With ΔG_{cav} being necessarily a positive quantity and ΔG_{el} quite generally negative, there is a possibility of cancellation of errors between ΔG_{cav} and the electrostatic term.

Quite generally, a larger cavity is expected to produce larger ΔG_{cav}. In the quantum mechanical approach to ΔG_{solv} by the polarizable continuum model [1], it has been observed that larger cavities cause more negative ΔG_{el} simply due to the increasing distance between the solute's nuclei and the ASC distributions. As a consequence, in implicit solvation models, the ASCs become more effected by the polarization of the surrounding dielectric. Our data from Table 1 indicate that larger ΔG_{cav} are not always accompanied by more negative ΔG_{el}. The use of shortest atom-solvent distances in our solvation

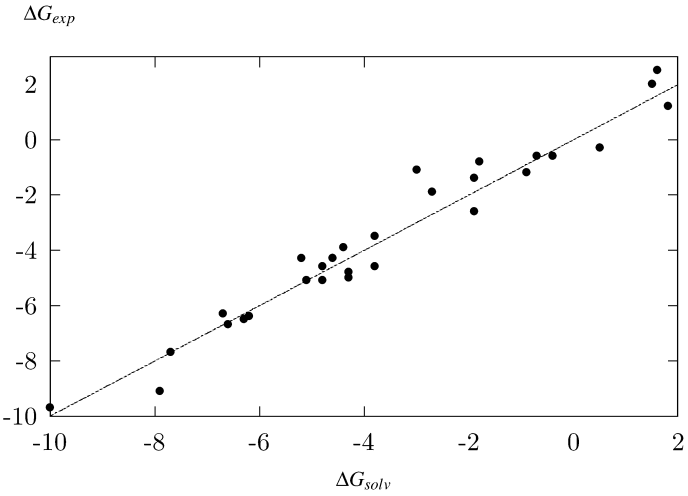

Fig. 1 Experimental free energies of solvation ΔG_{exp} against calculated free energies of solvation ΔG_{solv} for the solvent water. The line represents an optical guideline for perfect correlation. The free energies are given in kcal/mol.

model introduces additional geometrical anisotropies in the cavity that are also reflected in more anisotropic ASC distributions defining ΔG_{el}.

Comparing ΔG_{cav} for some of solutes listed in Table 1, one notes several inconsistencies in correlating the solute's size with the cavitational free energy. As an example, we cite the series of acids: acetic acid (ΔG_{cav} = 10.2 kcal/mol), propanoic acid (ΔG_{cav} = 9.1 kcal/mol), and butanoic acid (ΔG_{cav} = 14.1 kcal/mol). Similar problems with the cavitational term obtained from the GEPOL cavities have already been observed in implicit solvation models for *n*-alcohols in water [23] and have been related to weaknesses in the GEPOL algorithm for the cavity creation.

In Table 2, we present our results for 19 solutes in DMSO. For this solvent, there are only a few experimental solvation free energies available. Although the DMSO molecule differs more from the spherical symmetry than water, the comparison of the computed and experimental free energies demonstrates that our solvation model predicts Δ_{solv} accurately within the error bar. However, the calculated ΔG_{solv} are more negative than the experimental free energies of solvation for the five solutes with available experimental data. Due to the lack of experimental data, we cannot conclude that any systematical error affects our solvation model as has been observed for the solvent benzene [4] composed by planar molecules. Comparing some ΔG_{cav} for molecules with similar chemical functionalities, the GEPOL cavities in liquid DMSO reflect the expected tendency in producing larger ΔG_{cav} for larger solutes (see, e.g., the alcohols in Table 2). Also comparing ΔG_{cav} with the results for water from Table 1 for common solutes, the cavitational contributions in Table 2 reflect the size effect of the solvent molecules.

For the solvent THF, we summarized our free energies of solvation in Table 3. Again, the few available experimental ΔG_{exp} are in good agreement with our computed ΔG_{solv}. The cavitational contribution is larger than for DMSO due to the increased radius for the THF molecule. Similar to the water case, inconsistencies in ΔG_{cav} are observed for THF, for example, in the series of *n*-alcohols.

Table 2 Calculated free energies of solvation ΔG_{solv} and their contributions from eq. 1 for the solvent DMSO. Also given are experimental free energies of solvation ΔG_{exp} [22], when available. ΔG_{solv} was calculated using $\varepsilon = 46.70$ [11] and the radius $r_s = 2.415$ Å [24] for DMSO. The free energies are in kcal/mol.

Solute	ΔG_{el}	ΔG_{sr}	ΔG_{cav}	ΔG_{solv}	ΔG_{exp}
1,4–Dioxan	–5.3 ± 0.3	–13.5 ± 0.5	13.5 ± 0.4	–5.8 ± 0.8	–4.90
2–Propanol	–8.2 ± 0.7	–8.0 ± 0.4	11.1 ± 0.4	–5.0 ± 0.5	–
Anisole	–10.2 ± 0.4	–13.9 ± 0.5	15.9 ± 0.2	–8.2 ± 0.7	–
Benzene	–5.3 ± 0.6	–12.4 ± 0.6	12.7 ± 0.3	–5.0 ± 0.1	–
Butanone	–4.0 ± 0.4	–14.0 ± 0.4	13.2 ± 0.5	–4.8 ± 0.5	–4.23
Diethyl ether	–6.1 ± 0.4	–12.3 ± 0.5	15.1 ± 0.2	–3.3 ± 0.1	–
Dimethyl ether	–6.4 ± 0.5	–8.6 ± 0.4	9.8 ± 0.5	–5.2 ± 0.2	–
Ethanol	–5.8 ± 0.3	–10.2 ± 0.3	10.4 ± 0.6	–5.7 ± 0.4	–5.52
Ethylbenzene	–5.5 ± 0.5	–15.7 ± 0.7	17.0 ± 0.3	–4.1 ± 0.5	–
Phenol	–11.4 ± 0.7	–10.9 ± 0.5	13.2 ± 0.6	–9.0 ± 0.4	–
Fluorobenzene	–6.7 ± 0.8	–12.1 ± 0.5	13.6 ± 0.7	–5.1 ± 0.5	–
m–Xylene	–5.8 ± 0.4	–15.0 ± 0.7	17.4 ± 0.4	–3.4 ± 0.3	–
n–Butanol	–8.4 ± 0.6	–11.2 ± 0.4	14.4 ± 0.4	–5.2 ± 0.3	–
n–Octane	–2.4 ± 0.4	–23.3 ± 0.6	22.7 ± 0.3	–3.0 ± 0.5	–2.84
n–Propanol	–7.2 ± 0.7	–9.6 ± 0.4	12.2 ± 0.4	–4.7 ± 0.6	–
p–Xylene	–5.8 ± 0.4	–14.6 ± 0.5	17.3 ± 0.2	–3.1 ± 0.5	–
Tetrahydrofuran	–9.0 ± 0.5	–9.1 ± 0.4	12.6 ± 0.5	–5.5 ± 0.7	–
Tetrahydropyran	–8.2 ± 0.5	–11.5 ± 0.6	14.2 ± 0.5	–5.5 ± 0.4	–
Toluene	–3.4 ± 0.3	–16.1 ± 0.5	14.9 ± 0.6	–4.6 ± 0.4	–4.42

Table 3 Calculated free energies of solvation ΔG_{solv} and their contributions from eq. 1 for the solvent THF. Also given are experimental free energies of solvation ΔG_{exp} [22], when available. ΔG_{solv} was calculated using $\varepsilon = 7.58$ [11] and the radius $r_s = 2.90$ Å [24] for THF. The free energies are in kcal/mol.

Solute	ΔG_{el}	ΔG_{sr}	ΔG_{cav}	ΔG_{solv}	ΔG_{exp}
1,4-Dioxan	–7.3 ± 0.4	–11.7 ± 0.4	14.7 ± 0.4	–4.3 ± 0.6	–5.17
2–Propanol	–8.7 ± 0.4	–13.6 ± 0.8	16.0 ± 0.4	–6.2 ± 0.2	
Anisole	–9.2 ± 0.4	–16.5 ± 0.8	17.0 ± 0.6	–8.6 ± 0.9	
Benzene	–6.1 ± 0.6	–12.9 ± 1.0	13.8 ± 0.7	–5.3 ± 0.3	
Butanone	–7.3 ± 1.0	–11.5 ± 0.9	14.8 ± 0.5	–4.0 ± 0.5	–4.54
Dichloromethane	–6.5 ± 0.6	–12.4 ± 0.8	12.9 ± 0.8	–6.0 ± 0.2	
Diethyl ether	–6.7 ± 0.8	–12.8 ± 0.8	15.8 ± 0.4	–3.7 ± 0.7	
Dimethyl ether	–6.4 ± 0.5	–12.3 ± 0.9	12.8 ± 0.5	–5.9 ± 0.1	
Ethanol	–6.5 ± 0.3	–12.8 ± 0.3	14.1 ± 0.7	–5.2 ± 0.4	–4.56
Ethylbenzene	–6.7 ± 0.6	–16.3 ± 0.5	17.9 ± 0.3	–5.1 ± 0.3	
Phenol	–9.1 ± 0.7	–14.2 ± 0.8	13.1 ± 0.8	–10.1 ± 0.2	
m–Xylene	–5.5 ± 0.4	–17.8 ± 0.5	18.9 ± 0.5	–4.4 ± 0.2	
n–Butanol	–9.8 ± 0.5	–13.7 ± 0.4	18.5 ± 0.4	–5.0 ± 0.2	
n–Octane	–7.1 ± 0.4	–15.9 ± 0.3	17.5 ± 0.4	–5.5 ± 0.2	–5.39
n–Pentanol	–10.0 ± 0.6	–11.1 ± 0.5	15.1 ± 0.9	–6.0 ± 0.3	
n–Propanol	–8.1 ± 4.1	–10.9 ± 0.5	14.4 ± 0.5	–4.5 ± 0.2	
p–Xylene	–5.7 ± 1.0	–16.9 ± 0.8	18.0 ± 0.2	–4.7 ± 0.7	
Tetrahydrofuran	–9.8 ± 0.5	–11.0 ± 0.5	14.1 ± 0.5	–6.7 ± 0.5	
Tetrahydropyran	–9.7 ± 0.6	–11.5 ± 0.6	15.3 ± 0.6	–5.9 ± 0.5	
Toluene	–7.4 ± 0.3	–13.5 ± 0.4	14.9 ± 0.7	–6.0 ± 0.6	–5.50

Finally, in Tables 4 and 5, we present the ΔG_{solv} obtained from simulations on diluted solutions in CS_2 and acetonitril, respectively. In both cases, a satisfactory agreement with the few experimental data has been achieved. Both solvent molecules are more rod-like than spherical. Thus, one would expect some difficulties in the computation of the cavitational contribution. CS_2 possesses a larger molecular radius than acetonitril. However, the computed cavitational contributions in acetonitril are significantly larger than in CS_2 and appear not to be correlated with the solvent's molecular radius. We relate this observation again to problems in the creation of the cavity by the GEPOL algorithm that are partially cancelled by the electrostatic contribution ΔG_{el} as mentioned above.

Table 4 Calculated free energies of solvation ΔG_{solv} and their contributions from eq. 1 for the solvent CS_2. Also given are experimental free energies of solvation ΔG_{exp} [22], when available. ΔG_{solv} was calculated using $\varepsilon = 4.75$ [11] and the radius $r_s = 2.55$ Å [24] for CS_2. The free energies are in kcal/mol.

Solute	ΔG_{el}	ΔG_{sr}	ΔG_{cav}	ΔG_{solv}	ΔG_{exp}
1,4-Dioxan	–4.7 ± 0.5	–12.5 ± 0.6	12.2 ± 0.8	–5.0 ± 0.6	–4.67
Ethanoic acid	–4.6 ± 0.2	–10.5 ± 0.5	11.2 ± 0.3	–3.9 ± 0.9	–2.98
Benzene	–9.0 ± 0.4	–6.1 ± 0.7	10.1 ± 0.4	–5.0 ± 0.8	
Butanone	–4.5 ± 0.6	–9.2 ± 0.4	11.5 ± 0.1	–2.1 ± 0.7	–3.85
Ethanol	–4.5 ± 1.0	–10.7 ± 0.6	11.5 ± 0.9	–3.7 ± 0.8	–2.95
Phenol	–8.8 ± 0.8	–11.3 ± 1.0	13.0 ± 0.5	–7.1 ± 0.9	–6.27
n–Octane	–6.8 ± 0.7	–14.8 ± 0.7	16.5 ± 0.4	–5.1 ± 0.3	–5.68
Tetrahydrofuran	–9.0 ± 0.2	–8.5 ± 0.5	11.7 ± 0.8	–5.8 ± 0.6	
Tetrahydropyran	–8.8 ± 0.8	–11.9 ± 0.8	14.8 ± 0.9	–5.9 ± 0.7	
Toluene	–6.1 ± 0.8	–9.2 ± 0.6	10.4 ± 0.5	–4.9 ± 0.4	–5.39

Table 5 Calculated free energies of solvation ΔG_{solv} and their contributions from eq. 1 for the solvent acetonitril. Also given are experimental free energies of solvation ΔG_{exp} [22], when available. ΔG_{solv} was calculated using $\varepsilon = 37.50$ [11] and the radius $r_s = 1.87$ Å [24] for acetonitril. The free energies are in kcal/mol.

Solute	ΔG_{el}	ΔG_{sr}	ΔG_{cav}	ΔG_{solv}	ΔG_{exp}
1,4-Dioxan	–7.4 ± 0.9	–12.9 ± 0.5	14.5 ± 0.6	–5.8 ± 0.4	–5.33
Anisole	–7.1 ± 0.4	–16.1 ± 0.8	15.7 ± 0.8	–7.5 ± 0.8	
Benzene	–6.0 ± 0.6	–12.0 ± 0.4	13.8 ± 0.4	–4.2 ± 0.9	
Butanone	–5.1 ± 0.5	–14.6 ± 0.7	14.5 ± 0.5	–5.2 ± 0.5	–4.73
Diethyl ether	–6.8 ± 0.5	–15.1 ± 0.3	17.7 ± 1.0	–4.2 ± 0.6	
Dimethyl ether	–6.3 ± 0.8	–11.9 ± 0.4	11.9 ± 0.7	–6.3 ± 0.5	
Ethanol	–6.2 ± 0.9	–10.6 ± 0.5	11.6 ± 1.0	–5.2 ± 0.7	–4.43
Phenol	–9.8 ± 0.4	–13.9 ± 0.5	14.7 ± 0.9	–9.0 ± 0.6	
n–Butanol	–8.3 ± 0.7	–12.6 ± 0.5	15.8 ± 0.8	–5.0 ± 0.2	
n–Octane	–4.8 ± 0.8	–18.7 ± 0.5	19.5 ± 0.6	–4.1 ± 0.7	–3.57
n –Propanol	–8.3 ± 0.9	–9.6 ± 0.8	13.7 ± 1.0	–4.2 ± 0.2	
Tetrahydrofuran	–8.7 ± 0.5	–12.3 ± 1.0	14.6 ± 0.7	–6.3 ± 0.8	
Tetrahydropyran	–8.1 ± 0.5	–13.0 ± 0.5	14.7 ± 0.5	–6.4 ± 0.6	
Toluene	–6.0 ± 0.7	–14.3 ± 0.3	15.1 ± 0.2	–5.2 ± 0.9	–4.68

The short-range contribution to the solvation free energy from Tables 1–5 reflect the number and type of interactions sites on the solvent molecules. Although depending somehow on the choice of the applied force fields, we believe that the numerical values for ΔG_{sr} are accurately obtained for the equil-

ibrated solutions modeled by interaction parameters for the solvents that have been established directed toward the equilibrium properties of the pure liquids.

CONCLUSIONS

In the present article, we have applied our methodology for the calculation of the solvation free energy [4,5] to MD simulations on a variety of diluted solutions in different solvents. Although few experimental data are available from the literature, our method is shown to predict the free energy of solvation within an accuracy of approximately ±1 kcal/mol for solutions of small molecules in the solvents water, DMSO, THF, CS_2, and acetonitril.

The simulations were performed using all atom force fields for the solute and the solvent molecules.

However, the adopted methodology to ΔG_{solv} assumes solvents composed by spherical molecules in the creation of the cavitation and the computation of the cavitational contribution to the free energy of solvation by the scaled particle theory [10]. In solvents composed by molecules with anisotropies in the molecular shape, this approach has led to some systematical deviations between experimental and theoretical solvation free energies [5]. Several inconsistencies in the cavitational term ΔG_{cav} are also observed in this study and affect also the electrostatic contribution ΔG_{el} obtained from the created cavities. In most cases, an error in the positive contribution ΔG_{cav} is partially compensated by the negative ΔG_{el}.

In summary, our approach to the free energy of solvation previously tested for the solvents water [4], CCl_4, $CHCl_3$, and benzene [5] has been extended to additional solvents. So far, our methodology has been applied to various solvents composed by small molecules with a broad variety of molecular shapes. Also, the tested solvents cover a broad range of dielectric constants. Thus, one might conclude that our approach represents a promising tool for computing free energies of solvation from MD computer simulations.

ACKNOWLEDGMENTS

The authors wish to acknowledge financial support from the Brazilian agencies FAPERGS (process AUX 00/0902.7) and CNPq (processes 521628/97-0 and 573296/1998-7).

REFERENCES

1. J. Tomasi and M. Pérsico. *Chem. Rev.* **94**, 2027 (1994); C. J. Cramer and D. G. Truhlar. *Chem. Rev.* **99**, 2161 (1999); M. Orozco and F. J. Luque. *Chem. Rev.* **100**, 4187 (2000).
2. P. A. Kollman. *Chem. Rev.* **93**, 2395 (1993).
3. T. P. Straatsma, H. J. C. Berendsen, J. P. M. Postma. *J. Chem. Phys.* **85**, 6720 (1986); A. Perlman. *J. Chem. Phys.* **98**, 1487 (1994) and *J. Comput. Chem.* **15**, 105 (1994).
4. P. F. B. Gonçalves and H. Stassen. *J. Comput. Chem.* **23**, 706 (2002).
5. P. F. B. Gonçalves and H. Stassen. *J. Comput. Chem.* Accepted for publication.
6. R. Bonaccorsi, C. Ghio, J. Tomasi. In *Studies in Physics and Theoretic Chemistry Vol. 21*, R. Carbò (Ed.), p. 407, Elsevier, Amsterdam (1982).
7. A. Ben-Naim. *J. Phys. Chem.* **82**, 792 (1978).
8. J. L. Pascual-Ahuir, E. Silla, J. Tomasi, R. Bonaccorsi. *J. Comput. Chem.* **8**, 778 (1987); E. Silla, I. Tuñón, J. L. Pascual-Ahuir. *J. Comput. Chem.* **12**, 1077 (1991); J. L. Pascual-Ahuir and E. Silla. *J. Comput. Chem.* **11**, 1047 (1990); E. Silla, F. Villar, O. Nilsson, J. L. Pascual-Ahuir, O. Tapia. *J. Mol. Graph.* **8**, 168 (1990).
9. P. Claverie. In *Intermolecular Interactions, from Diatomics to Biomolecules*, B. Pullman (Ed.), p. 69, Wiley, Chichester (1978).

10. R. A. Pierotti. *Chem. Rev.* **76**, 717 (1976).
11. D. R. Lide (Ed.). *Handbook of Chemistry and Physics,* 80th ed., CRC Press, Boca Raton (1999–2000).
12. I. Tironi, R. Sperb, P. Smith, W. F. van Gunsteren. *J. Chem. Phys.* **102**, 5421 (1995).
13. M. P. Allen and D. J. Tildesley. *Computer Simulation of Liquids*, Clarendon Press, Oxford (1987).
14. S. Nosé. *Mol. Phys.* **51**, 255 (1984).
15. F. M. Floris, J. Tomasi, J. L. Pascual-Ahuir. *J. Comput. Chem.* **12**, 784 (1991).
16. M. J. Frisch, G. W. Trucks, H. B. Schlegel, G. E. Scuseria, M. A. Robb, J. R. Cheeseman, V. G. Zakrzewski, J. A. Montgomery Jr., R. E. Stratmann, J. C. Burant, S. Dapprich, J. M. Millam, A. D. Daniels, K. N. Kudin, M. C. Strain, O. Farkas, J. Tomasi, V. Barone, M. Cossi, R. Cammi, B. Mennucci, C. Pomelli, C. Adamo, S. Clifford, J. Ochterski, G. A. Petersson, P. Y. Ayala, Q. Cui, K. Morokuma, D. K. Malick, A. D. Rabuck, K. Raghavachari, J. B. Foresman, J. Cioslowski, J. V. Ortiz, A. G. Baboul, B. B. Stefanov, G. Liu, A. Liashenko, P. Piskorz, I. Komaromi, R. Gomperts, R. L. Martin, D. J. Fox, T. Keith, M. A. Al-Laham, C. Y. Peng, A. Nanayakkara, M. Challacombe, P. M. W. Gill, B. Johnson, W. Chen, M. W. Wong, J. L. Andres, C. Gonzalez, M. Head-Gordon, E. S. Replogle, J. A. Pople. Gaussian Inc., Pittsburgh (1998).
17. W. L. Jorgensen and J. Tirado-Rives. *J. Am. Chem. Soc.* **110**, 1657 (1988); D. S. Maxwell, J. Tirado-Rives, W. L. Jorgensen. *J. Comput. Chem.* **16**, 984 (1995); G. Kaminski, E. M. Duffy, T. Matsui, W. L. Jorgensen. *J. Phys. Chem.* **98**, 13077 (1994).
18. H. Liu, F. Müller-Plathe, W. F. van Gunsteren. *J. Am. Chem. Soc.* **117**, 4363 (1995).
19. D. J. Tildesley and P. A. Madden. *Mol. Phys.* **42**, 1142 (1981).
20. H. J. C. Berendsen, J. R. Grigera, T. P. Straatsma. *J. Phys. Chem.* **91**, 6269 (1987).
21. C. G. Gray and K. E. Gubbins. *Theory of Molecular Fluids, Vol. 1: Fundamentals*, Clarendon Press, Oxford (1984).
22. G. D. Hawkins, C. J. Cramer, D. G. Truhlar. *J. Phys. Chem. B* **102**, 3257 (1998, supporting information).
23. A. A. C. C. Pais, A. Sousa, M. E. Eusébio, J. S. Redinha. *PCCP* **3**, 4001 (2001).
24. We have used the solvent radii as defined within the Gaussian98revA9 program [16].